Interaction of Mithramycin with DNA Fragments Complexed with Nucleosome Core Particles: Comparison with Distamycin and Echinomycin†

Keith R. Fox* and Benjamin M. G. Cons

Department of Physiology and Pharmacology, University of Southampton, Bassett Crescent East, Southampton SO9 3TU, U.K.

Received February 19, 1993

ABSTRACT: We have studied the sequence-specific interaction of mithramycin with nucleosome core particles which have been reconstituted with various DNA fragments. Mithramycin binds to these DNAs without disrupting the integrity of the nucleosome and produces clear DNase I footprints centered around GC-rich regions. In some instances, the footprints produced on free DNA are resolved into two or more smaller sites when the DNA is complexed with the nucleosome core. In a few cases, novel footprints are produced in sequences which did not bind the drug in free DNA samples. The results are explained by suggesting mithramycin binds to GC-rich regions in which the minor groove faces away from the protein core, and which possess a wider than normal narrow groove on account of their location. Hydroxyl radical footprinting and diethyl pyrocarbonate modification confirm that mithramycin does not affect the rotational positioning of the nucleosome-bound DNA. Although distamycin and echinomycin induce novel DNase I digestion products in nucleosomal DNA which are consistent with the proposed change in DNA positioning [Low, C. M. L., Drew, H. R., & Waring, M. J. (1986) *Nucleic Acids Res. 14,* 6785–6801], hydroxyl radical footprinting and diethyl pyrocarbonate modification suggest these ligands do not change the rotational positioning of the DNA on the nucleosome cores.

The antitumor antibiotic mithramycin acts by binding to DNA (Kersten et al., 1966; Gause, 1975) in a reaction requiring stoichiometric quantities of divalent metal ions, especially magnesium (Cons & Fox, 1989b). Various footprinting studies have shown that the ligand, together with the related compounds chromomycin and olivomycin, binds to GC-rich regions of DNA, especially runs of at least three contiguous GC pairs (Van Dyke & Dervan, 1983; Fox & Howarth, 1985; Con & Fox, 1989b). Although the antibiotic binds to the dinucleotide GpG, the presence of two adjacent GC residues is not necessarily sufficient. NMR studies failed to detect binding to an oligonucleotide with a single CpG site (Banville et al., 1990a) while DNase I and hydroxyl radical footprints are not observed at all potential binding sites, even at some which contain three contiguous GC base pairs (Cons & Fox, 1989b).

Several NMR studies have shown that mithramycin binds as a dimer, coordinating a single magnesium ion, within the DNA minor groove (Gao & Patel, 1989, 1990; Gao et al., 1992; Banville et al., 1990a,b). The DNA is highly distorted around the binding site so that the wide minor groove more closely resembles an A-DNA helix. This large structural distortion may account for the observation that mithramycin binding is affected by the surrounding sequences. Although mithramycin does not unwind DNA (Waring, 1970), it alters the local DNA structure, rendering adjacent runs of $(AT)_n$ and $A_n{\cdot}T_n$ more sensitive to digestion by DNase I (Cons & Fox, 1991) and regions of $(AT)_n$ to digestion by DNase II (Cons & Fox, 1990a).

Although there is much information on the interaction of mithramycin with isolated DNA fragments, this does not necessarily correspond to the situation present within eukaryotic cells in which the DNA is complexed with histones and many other proteins. These may affect the DNA structure and accessibility and modify its interaction with mithramycin. Nonetheless it has been suggested that mithramycin inhibits RNA polymerase by binding to GC-rich sequences in eukaryotic promoters and thereby prevents the binding of regulatory proteins such as Sp1 (Ray et al., 1989; Snyder et al., 1991).

Several studies have established that DNA is not randomly positioned on nucleosome core particles but adopts a preferred orientation (Drew & Travers, 1985; Drew & Calladine, 1987; Hayes et al., 1990a,b, 1991; Schrader & Crothers, 1989, 1990). The precise rotational orientation is determined by the local DNA sequence, affecting its flexibility and curvature. Where the minor groove is wide (typically GC-rich), it faces away from the protein core, whereas narrow minor grooves (typically AT-rich) face toward the core. Within each DNA fragment, it will not be possible to satisfy all the local preferences, and the exact positioning will reflect the sum of all the local preferences. Since DNA positioning is determined by its structure, we might expect that ligands which distort the DNA helix will alter the way in which its interacts with the nucleosome. Indeed, several studies from Waring's laboratory have suggested that both the bifunctional intercalator echinomycin and several groove binding ligands cause DNA to rotate by 180° on the protein core (Low et al., 1986; Portugal & Waring, 1987a). In the presence of these ligands, new DNase I digestion products appear which are located midway between the maxima seen in the digestion of the core particles alone. In contrast, the intercalators actinomycin and nogalamycin cause DNA to dissociate from the core particles (Portugal & Waring, 1986).

In this study, we have examined the interaction of mithramycin with several DNA fragments which have been complexed with nucleosome core particles. This has been achieved using a variety of footprinting probes including DNase I, hydroxyl radicals, and diethyl pyrocarbonate. The results are compared with those for distamycin and echinomycin.

† This work was supported by grants from the Cancer Research Campaign and the Science and Engineering Research Council. K.R.F. is a Lister Institute Research Fellow.

* To whom correspondence should be addressed. Telephone: 0703–594374. FAX: 0703–594319.

0006-2960/93/0432-7162$04.00/0

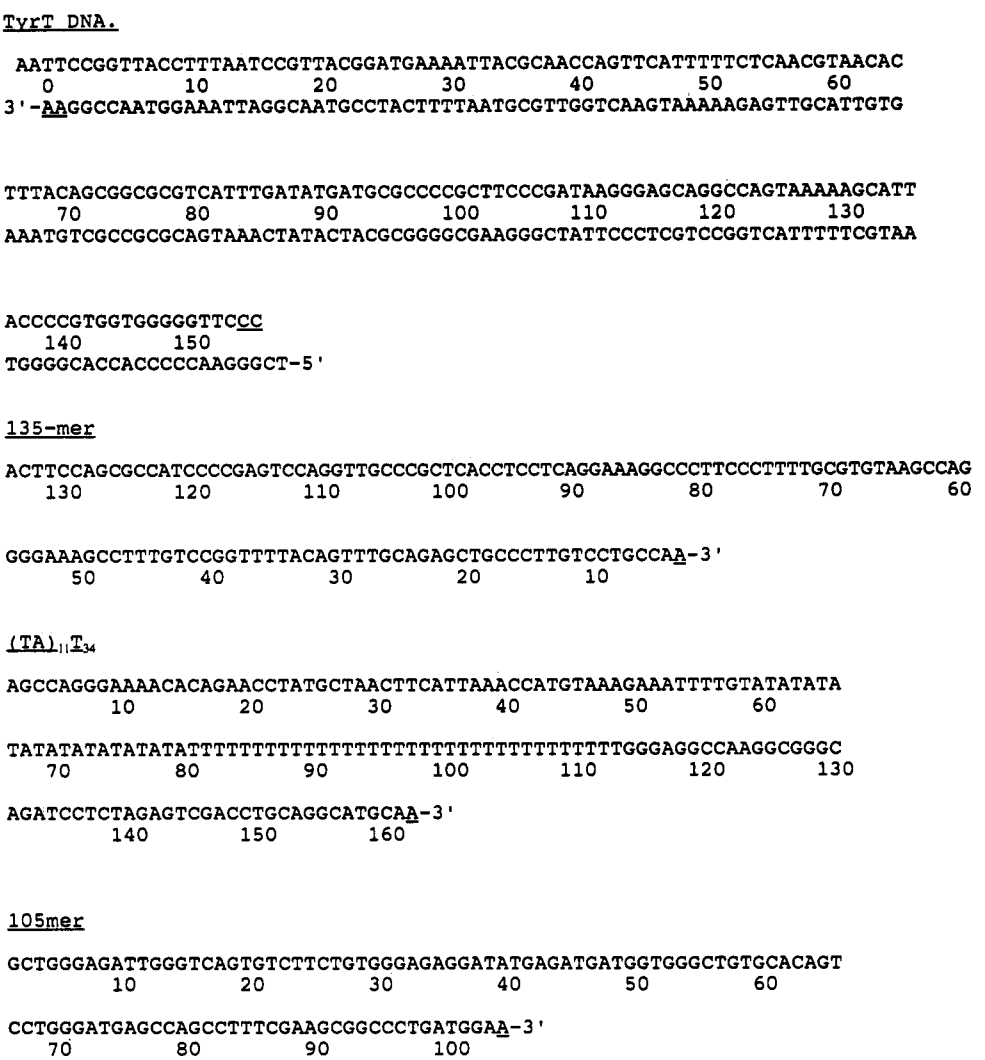

FIGURE 1: Sequences of DNA fragments. The bases bearing the radioactive phosphates are underlined.

MATERIALS AND METHODS

Drugs and Enzymes. Mithramycin was a gift from Pfizer and was stored at 4 °C as a 2 mM stock solution in 10 mM Tris-HCl, pH 8.0, containing 10 mM NaCl. Distamycin was purchased from Sigma. Echinomycin was supplied by the Drug Synthesis and Chemistry Branch, National Cancer Institute. DNase I was purchased from Sigma and stored as previously described (Fox & Waring, 1984).

DNA Fragments. The *tyr*T DNA fragment was isolated from plasmid pKMΔ-98 as previously described by digesting with *Eco*RI and *Ava*I (Fox & Waring, 1984; Low et al., 1986). This was labeled at the 3′-end of the *Eco*RI site with [α-^{32}P]-dATP or at the *Ava*I site with [α-^{32}P]dCTP using reverse transcriptase. The 135 base pair fragment was obtained from pXbs1 as previously described by digesting with *Hin*dIII and *Sau*3A1 and labeled at the 3′-end of the *Hin*dIII site with [α-^{32}P]dATP using reverse transcriptase (Cons & Fox, 1989b). The 160 and 105 base pair fragments were obtained from the human genomic clone k2 (Fox, 1992) which contains the sequence $(TA)_{11}T_{34}$. The cloned sequence contains an internal *Hin*dIII site so that digestion with *Hin*dIII and *Fnu*4H1 followed by labeling with [α-^{32}P]dATP using reverse transcriptase yielded two fragments of 105 and 161 base pairs, the longer of which contains the sequence $(TA)_{11}T_{34}$. The DNA fragments of interest were separated from the remainder of the plasmid on 6% polyacrylamide gels. The sequences of these DNAs are presented in Figure 1.

Reconstitution of Nucleosome Core Particles. Nucleosome core particles derived from chicken erythrocytes were prepared as previously described (Drew & Travers, 1985; Drew & Calladine, 1987) and stored at −20 °C in 50% glycerol. The DNA fragments were reconstituted onto the nucleosomes by salt exchange as previously described (Drew & Travers, 1985; Drew & Calladine, 1987; Fox, 1992) by incubating the labeled DNA with 50 μg of nucleosome core particles in a high-salt buffer. The salt concentration was slowly decreased to 70 mM by stepwise additions of 5 mM Tris-HCl, pH 8.0, containing 1 mM EDTA and 0.1% (v/v) Nonidet P40. Incorporation of the DNA onto the nucleosome cores was checked by retardation on agarose gels and was found to be greater than 95% in every case.

Digestion of Nucleosome Core Particles. Nucleosome core particles were digested with DNase I as previously described (Drew & Travers, 1985; Low et al., 1986; Fox, 1992). All reactions contained 1 mM $MgCl_2$, necessary both for DNase I activity and for mithramycin binding. Hydroxyl radical cleavage was achieved by mixing 10 μL of reconstituted core particles (made fresh, containing no glycerol) with 2 μL of mithramycin and digesting with a freshly prepared mixture containing 50 μM ferrous ammonium sulfate, 100 μM EDTA, 2 mM ascorbic acid, and 0.01% hydrogen peroxide. The reaction was stopped after 10 min by addition of 4 μL of 100 mM thiourea. The mixture was extracted twice with phenol and precipitated as described for DNase I. Modification by

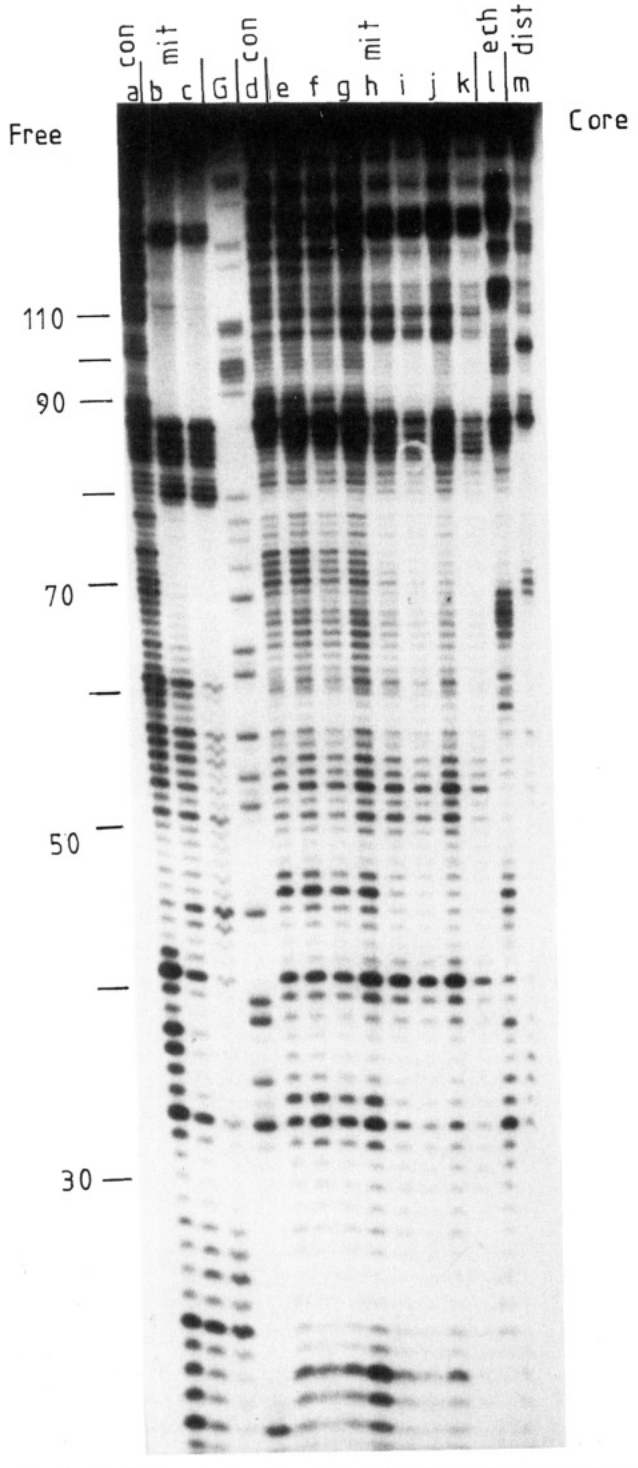

FIGURE 2: DNase I digestion of *tyr*T DNA, labeled at the 3′-end of the *Eco*RI site (bottom strand in Figure 1), both free and complexed with nucleosome core particles in the presence of mithramycin, distamycin, and echinomycin. Lanes a–c, free DNA; d–m, reconstituted core particles. Tracks a and d (con) are controls in the absence of added ligand. The mithramycin concentrations were 2 (e), 5 (f), 10 (g), 20 (h), 50 (b, i), 100 (c, j), and 200 μM (k). Lane l contains 50 μM echinomycin; lane m contains 20 μM distamycin. The numbering corresponds to the sequence shown in Figure 1. The track labeled "G" is a Maxam–Gilbert dimethyl sulfate–piperidine marker specific for guanine.

diethyl pyrocarbonate (DEPC) was achieved by adding 5 μL of DEPC to 10 μL of reconstituted cores. The mixture was terminated after 5 min by extracting with phenol. After precipitation with ethanol, the DNA was cleaved by boiling in 10% piperidine and subsequently lyophilized.

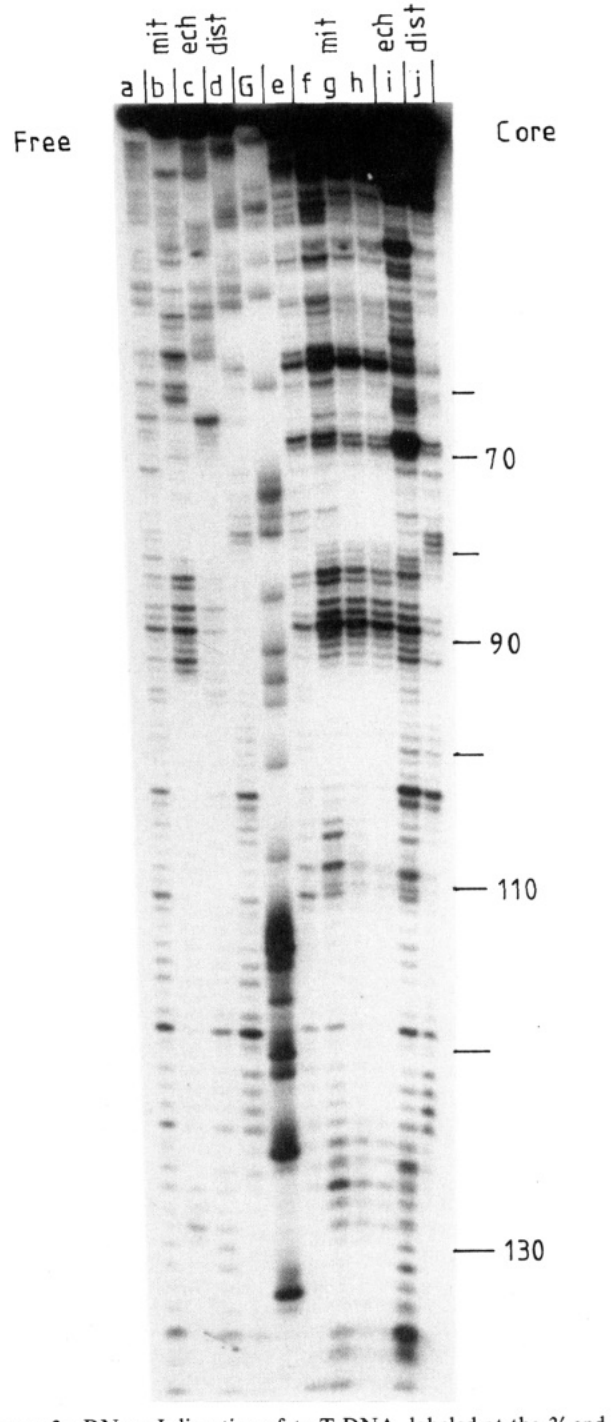

FIGURE 3: DNase I digestion of *tyr*T DNA, labeled at the 3′-end of the *Ava*I site (top strand in Figure 1), both free and complexed with nucleosome core particles in the presence of mithramycin, distamycin, and echinomycin. Lanes a–d, free DNA; e–j, reconstituted core particles. Tracks a and e are controls in the absence of added ligand. The mithramycin concentrations were 5 (f), 50 (b, g), and 100 μM (h). Lanes c and i contain 50 μM echinomycin; lanes d and j contain 20 μM distamycin. The track labeled "G" is a Maxam–Gilbert dimethyl sulfate–piperidine marker specific for guanine.

Electrophoresis. Products of the DNA cleavage reactions were dissolved in 80% formamide containing 10 mM EDTA, 10 mM NaOH, and 0.1% bromophenol blue. Samples were boiled for 3 min before being loaded onto 40-cm-long 8% polyacrylamide gels containing 8 M urea. Electrophoresis was carried out for about 2 h at 1500 V. After electrophoresis, gels were fixed in 10% acetic acid, transferred to Whatmann 3MM paper, dried under vacuum at 80 °C, and exposed to autoradiography at −70 °C with an intensifying screen.

Autoradiographs of hydroxyl radical cleavage were scanned with a Joyce-Loebl chromoscan 3 microdensitometer.

RESULTS

TyrT DNA. Patterns of DNase I digestion of *tyr*T DNA, both free and complexed with nucleosome core particles, in the presence of various concentrations of mithramycin are presented in Figure 2 for DNA labeled at the 3′-end of the *Eco*RI site (bottom strand of the sequence shown in Figure 1) and in Figure 3 for DNA labeled at the 3′-end of the *Ava*I site (top strand of the sequence shown in Figure 1). DNase I footprints for mithramycin on this DNA fragment have been described by Fox and Howarth (1985). DNase I digestion of the core-bound DNA, in the absence of the antibiotic, reveals a distribution of products which is modulated relative to that of the free DNA with a periodicity of about 10 base pairs (Drew & Travers, 1985). On the bottom strand (Figure 2), bands in the core lane are missing at positions 24–28, 36–39, 58–60, and 74–78. Simiarly, for the top strand (Figure 3), bands are missing at positions 70–74, 100–104, and 114–118, with new cleavage products at positions 56, 59, 76, 89, 108, 119, and 127. These results are similar to those reported by Drew and Travers (1985). The previous studies rigorously assigned the orientation of this DNA relative to the protein core and showed that the minor groove faces toward the protein at positions 18, 28, 39, 49, 60, 70, 80, 90, 100, 112, 121, and 131 while positions 13, 23, 33, 44, 55, 65, 74, 84, 94, 105, 116, and 126 lie on the outer surface.

The digestion is modified by mithramycin, yielding patterns which are different from both the drug-free core sample and free DNA in the presence or absence of drug. Two conclusions can immediately be drawn. First, mithramycin has not caused the DNA to dissociate from the core particles since the mithramycin-treated free and core samples reveal different cleavage patterns. Second, the presence of clear footprints indicates that mithramycin is able to bind to the core-bound DNA in a sequence-selective fashion.

Looking first at the labeled bottom strand (Figure 2), it can be seen that mithramycin, at concentrations of 20 μM and above, protects the core-bound DNA from cleavage in three distinct regions around positions 70–80, 93–101, and 115–120. Each of these corresponds to similar blockages seen with the free DNA (Fox & Howarth, 1985) and represents binding to guanine-rich sequences. However, the patterns of protection are not the same for free and core-bound DNA samples. On the free DNA, mithramycin produces a large footprint between 91 and 120, which is resolved into two discrete footprints on the core-bound DNA; the bands between 103 and 113 are protected from cleavage in the free but not the core-bound DNA.

A similar effect is seen on the labeled top strand (Figure 3). On the core DNA, mithramycin produces three clear footprints at positions 70–80, 93–102, and 111–123, compared with two on the free DNA at positions 70–80 and 92–123. The single blockage at 92–123 has again been resolved into two discrete sites; bands between 103 and 110 are not protected from cleavage on the core-bound DNA. The region between 93 and 120 is very GC-rich (70%) so that the potential mithramycin binding sites overlap, producing a single large footprint on free DNA. It appears that some of these sites are unavailable in the core-bound DNA, either because of their structure or due to steric occlusion from the protein.

Previous studies (Fox & Howarth, 1985) have shown enhanced DNase I cleavage in the presence of mithramycin around position 80, which is most evident on the labeled bottom strand (Figure 2, lanes b and c). These enhancements are not apparent in the core-bound samples, possibly because this is a region where cleavage is already reduced since the DNA minor groove faces toward the protein core. In contrast to the results reported for echinomycin and distamycin (Low et al., 1986), no novel cleavage products are evident in the mithramycin-treated core samples. Examples of these can be seen in the echinomycin- and distamycin-treated lanes presented in Figures 2 and 3 and are similar to those previously reported. These enhancements are clearest on the labeled upper strand (Figure 3) and can be seen at positions 62, 70–72, 78–80, 92, 103–104, and 124–125. These lie approximately five bases away from those sites which are cut best in the drug-free core DNA at positions 56, 69, 76, 89, 108, and 119. Low et al. attributed these effects to a drug-induced change in the orientation of the DNA with respect to the protein core.

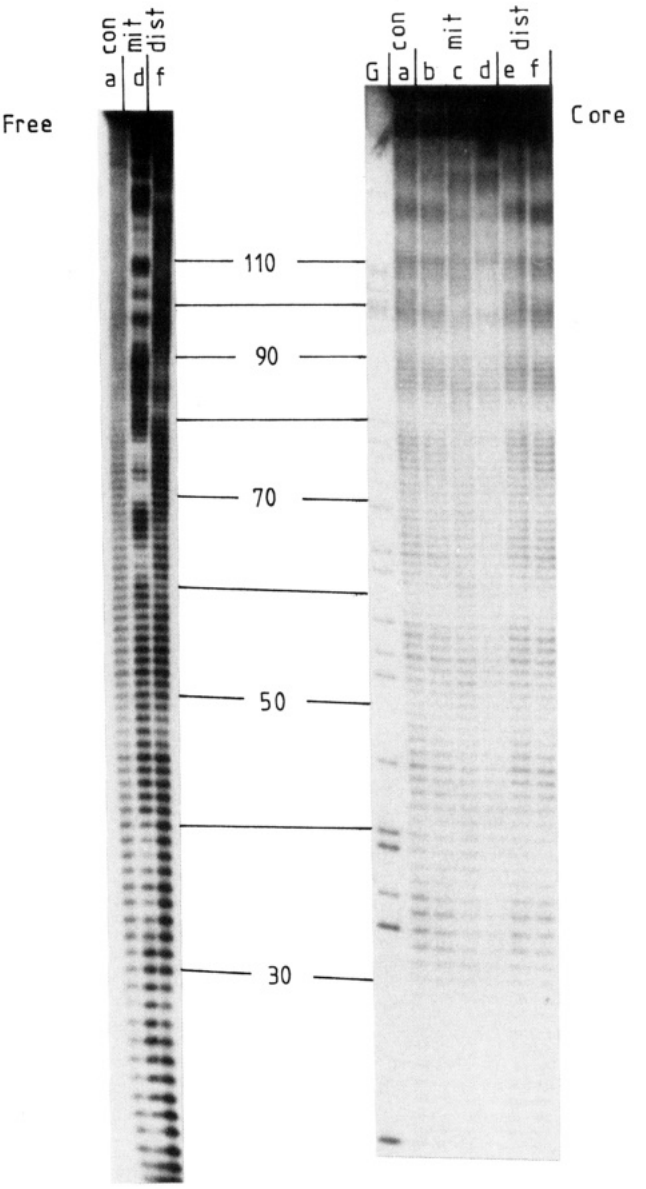

FIGURE 4: Hydroxyl radical cleavage of *tyr*T DNA, labeled a the 3′-end of the *Eco*RI site, both free and complexed with nucleosome cores, in the presence and absence of mithramycin and distamycin. The three lanes on the left show the digestion of free DNA; the lanes on the right correspond to digestion of core-bound DNA. The tracks are labeled as follows: a (con), control; b, c, and d, mithramycin at concentrations of 5, 50, and 100 μM, respectively; e and f, distamycin (2 and 20 μM, respectively). The track labeled "G" is a Maxam–Gilbert dimethyl sulfate–piperidine marker specific for guanine.

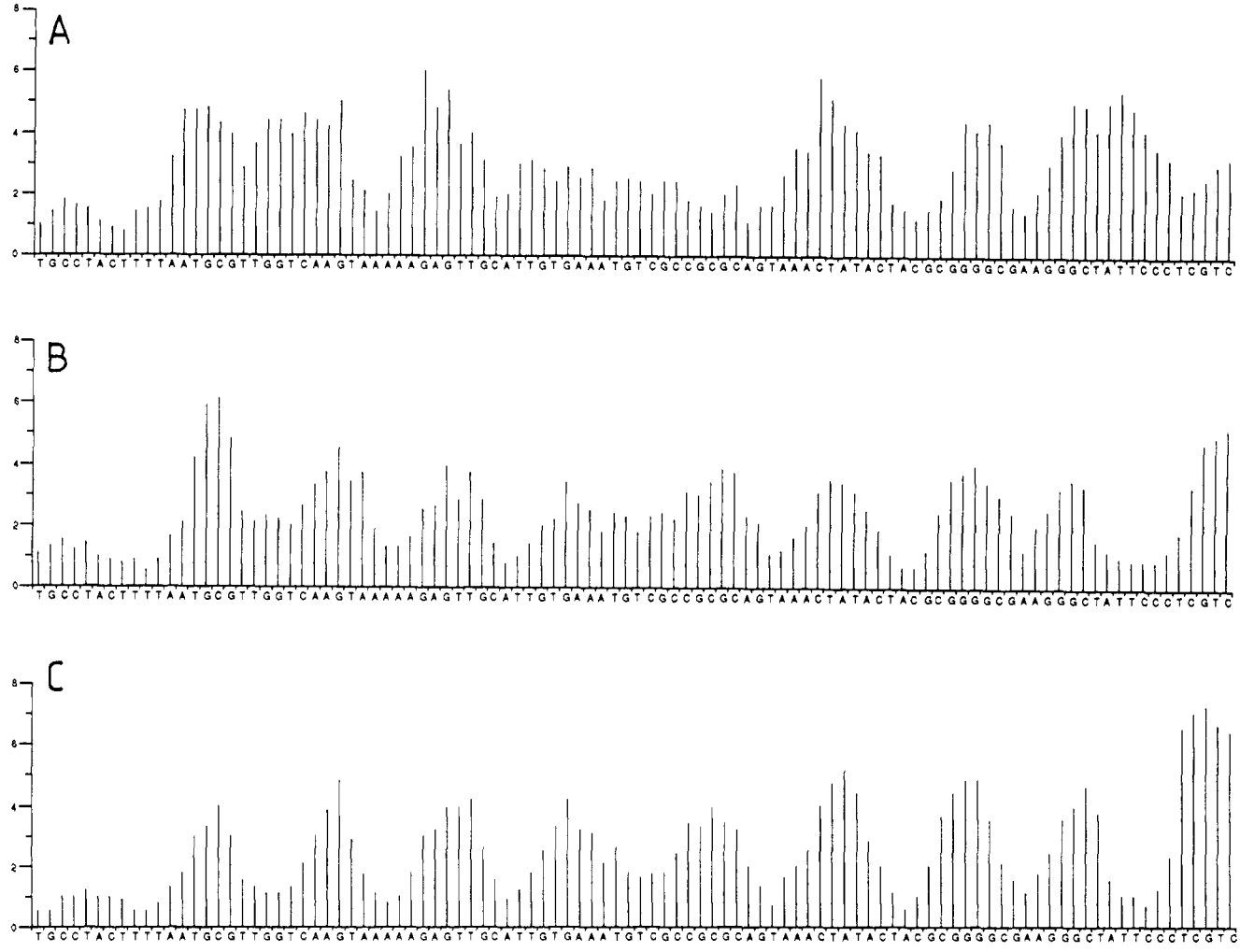

FIGURE 5: Histograms representing hydroxyl radical cleavage of core-bound *tyr*T DNA in the presence and absence of mithramycin and distamycin. (A) 50 μM mithramycin; (B) control; (C) 25 μM distamycin. The data are derived from densitometer traces of the autoradiographs shown in Figure 4.

Another contrast between these two ligands and mithramycin is that the two former ligands do not produce clear footprints in the nucleosomal DNA (Low et al., 1986) whereas mithramycin generates distinct footprints.

In order to define more rigorously the effect of mithramycin on these core particles, we have used hydroxyl radical footprinting to map the changes at higher resolution. Distamycin was also included in these studies for comparison: echinomycin cannot be studied in this way as it is only sparingly soluble in water and is dissolved in dimethyl sulfoxide which quenches the free radical reaction. Although the binding of mithramycin to this fragment has previously been assessed by DNase I footprinting (Cons & Fox, 1989b), this is the first report of hydroxyl radical cleavage of nucleosome-bound *tyr*T DNA; the results for the drug-free control will therefore be described first.

Figure 4 presents hydroxyl radical cleavage patterns of nucleosome-bound *tyr*T DNA in the presence and absence of mithramycin and distamycin. These data are presented more clearly as histograms, derived from densitometer traces of these lanes, in Figure 5. Digestion of the free DNA produces an even ladder of bands (Cons & Fox, 1989b; Portugal & Waring, 1987c). Digestion of the drug-free core-bound samples produces a pattern which is clearly phased, with a repeat of about 10 base pairs. Minima in the cleavage pattern are located at positions 29, 39, 50, 59, 81, 93, 102, and 112, close to the minima for DNase I cleavage at positions 25, 37, 48, 58, 68, 77, 90, 99, and 110 (Drew & Travers, 1985). The DNase I minima are each staggered between 1 and 3 bases in the 3′-direction relative to the hydroxyl radical data. Between positions 35 and 119, the pattern reveals 8 maxima, suggesting a periodicity of 84/8, i.e., 10.5 base pairs per turn. There is a break in the regular pattern around positions 65–75, presumably because this corresponds to the nucleosome dyad.

Inspection of the hydroxyl radical cleavage of core-bound DNA in the presence of mithramycin reveals that, although the pattern has been modified by the ligand, there are no major changes in the phasing. Clear minima are found at positions 27, 37, 48, 58, 93, 102, and 115, one or two bases to either side of the minima in the drug-free control. It is not possible to determine the position of the bound mithramycin molecules from these hydroxyl radical data since there are no clear footprints, even in regions which were protected from DNase I cleavage. It can be seen that the phasic nature of the cleavage pattern is less pronounced in the presence of mithramycin, suggesting that the regions which are normally more accessible to hydroxyl radical attack are protected by the antibiotic.

Histograms showing hydroxyl cleavage of nucleosome-bound *tyr*T DNA in the presence of distamycin are also presented in Figure 5. These reveal few antibiotic-induced changes with maxima and minima located at the same positions. It is clear from these data that distamycin has not

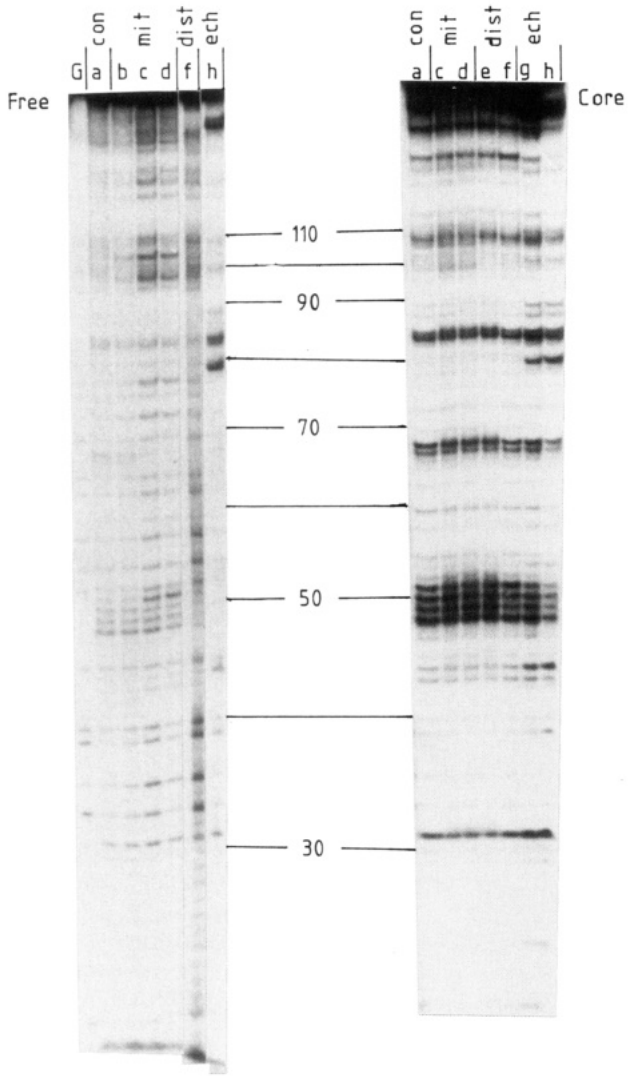

FIGURE 6: Pattern of DEPC-mediated cleavage of *tyr*T DNA, labeled at the 3′-end of the *Eco*RI site, in the presence of mithramycin, distamycin, and echinomycin. The tracks in the left panel correspond to the free DNA; those in the right panel represent the nucleosome-bound DNA. Tracks are labeled as follows: a (con), control; b, c, and d, mithramycin (5, 50, and 100 μM, respectively); e and f, distamycin (2 and 20 μM, respectively); g and h, echinomycin (5 and 50 μM, respectively). The track labeled "G" is a Maxam–Gilbert dimethyl sulfate–piperidine marker specific for guanine.

altered the positioning of *tyr*T DNA on the core particles; if anything, the phasic pattern is more intense in the presence of the ligand, especially around the dyad (position 70). This may be because many of the minima correspond to AT-rich regions, such as 30 (TTTTAAT), 50 (AAAAA), 60 (ATTGT), 80 (AGTAAA), 102 (GAAG), and 112 (TATT), each of which corresponds to distamycin binding sites (Portugal & Waring, 1987b).

Several studies have shown that diethyl pyrocarbonate can detect drug-induced changes in DNA structure (Mendel & Dervan, 1987; Portugal et al., 1988; Fox & Kentebe, 1990). This agent has been shown to produce a phased cleavage pattern in nucleosome-bound tracts of $A_n \cdot T_n$ which is out of phase with DNase I cleavage maxima and corresponds to regions where the DNA major groove faces away from the protein core (Fox, 1992). We have therefore used this probe to investigate the interaction of these ligands with core-bound DNA. Figure 6 presents the DEPC-mediated cleavage of nucleosome-bound *tyr*T DNA in the presence and absence of mithramycin, distamycin, and echinomycin. Although cleavage of the free DNA is weak, several bases in the core-bound DNA exhibit increased reactivity to DEPC. These strong cleavage products are all at adenines and are located at positions 31, 48–51, 66–67, and 83–84. Each of these corresponds to an AT-rich region where the minor groove is proposed to face toward the histone octamer; i.e., the major groove faces away from the core. Presumably these regions have a slightly modified DNA structure, relative to that found in free DNA, which renders them more accessible to DEPC. Mithramycin causes no changes in the pattern of DEPC cleavage. This is not surprising since mithramycin does not affect DEPC-mediated cleavage of free DNA (Cons & Fox, 1990b), but again demonstrates that the ligand has not caused any major changes in the structure of the nucleosome-bound DNA. Similarly, distamycin has no effect on DEPC-mediated cleavage of the core-bound DNA, again suggesting that the drug does not alter the rotational positioning of the DNA on the protein core. In the presence of echinomycin, new DEPC cleavage products are evident at several adenines in the core-bound DNA. These are found at positions 44 (TGA), 79 (TGA), 87 (ATA), and 89 (TCA) in identical positions to the sites of echinomycin-induced DEPC cleavage of free DNA (Portugal et al., 1988). This demonstrates two important features. First, the structural changes produced by bifunctional intercalation of echinomycin can be tolerated within the nucleosome core particle. Second, these changes are superimposed on the DEPC-mediated cleavage pattern of drug-free core-bound DNA, suggesting that echinomycin has not radically altered the way in which this sequence interacts with the protein core. These changes will be considered further under Discussion.

135mer. DNase I digestion patterns of nucleosome-bound 135mer in the presence and absence of mithramycin are presented in Figure 7, together with examples of the cleavage in the presence of echinomycin and distamycin. Cleavage of the core-bound DNA yields a distribution of product lengths which is modulated with a periodicity of about 10 base pairs as previously reported (Drew & Calladine, 1987; Portugal & Waring, 1987). The strongest cleavage in this core-bound DNA can be seen around positions 60, 70, 90, and 100. This pattern is modified by mithramycin in a concentration-dependent fashion, generating regions of reduced DNase I cleavage around positions 44–47, 50–57, 60–63, 71–74, and 88–92. This pattern is not the same as that observed with free DNA for which larger footprints are found around positions 36–41, 44–58, 71–83, and 90–110. This difference emphasizes that mithramycin has not displaced the DNA from the core particles. The single protection between 44 and 58 has been resolved into two smaller binding sites on the core-bound DNA, while the blockage between 71 and 83 is restricted to the lower portion of this site. A novel footprint is found on the core DNA around 60–63 which was not evident with the free DNA and possibly corresponds to interaction of mithramycin with GCC. Mithramycin causes increased DNase I cleavage of the core-bound DNA at positions 31, 42, 59, 64, 82, 88, and 111. In general, these new bands correspond to regions of enhanced cleavage produced by the ligand in free DNA (lane b; Cons & Fox, 1989b). These new bands are found at various distances from the bands which are cut well in the control core particles, suggesting that mithramycin has not induced any rotation of the DNA on the core particles, in contrast to the results reported for echinomycin and distamycin (Portugal & Waring, 1987a). Examples of these can be seen in the echinomycin- and distamycin-treated lanes in Figures 6. With echinomycin, conspicuous new bands appear around positions

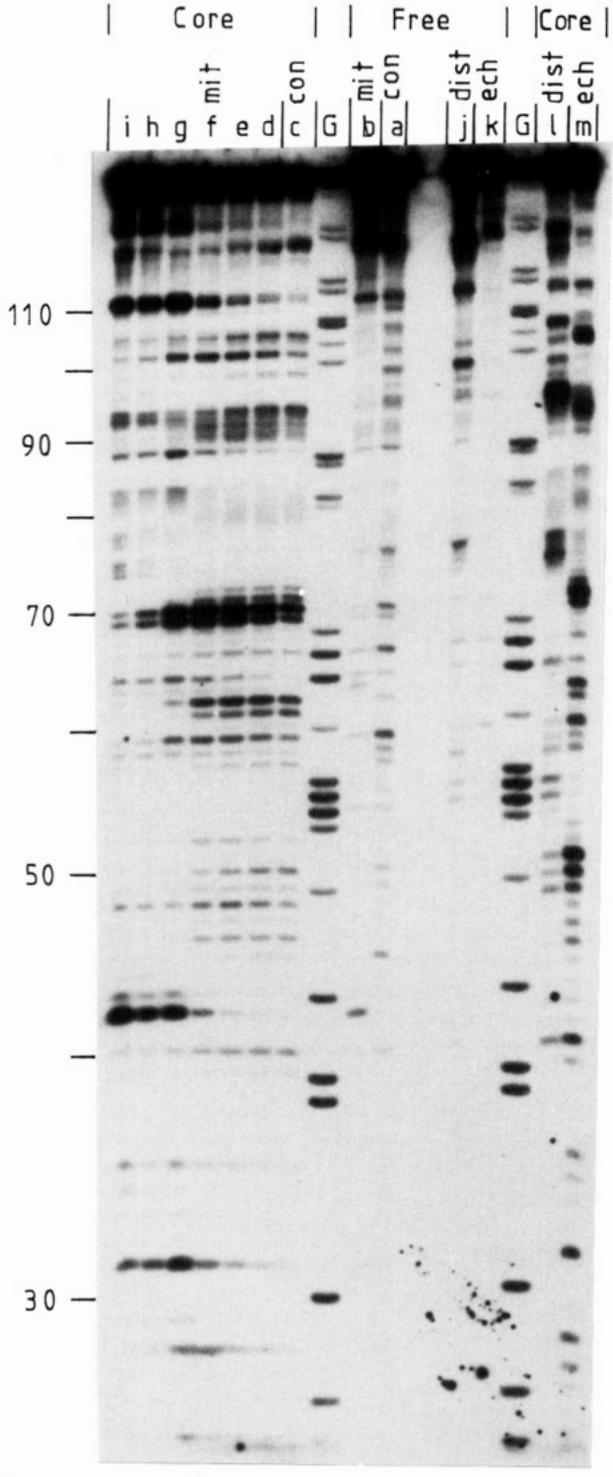

FIGURE 7: Patterns of DNase I digestion of the 135-mer, both free and complexed with nucleosome core particles, in the presence and absence of mithramycin, distamycin, and echinomycin. Lanes a, b, j, and k correspond to the free DNA; the remainder represents the core-bound DNA. Tracks a and c (con) are controls in the absence of antibiotic. The mithramycin concentrations were 1 (d), 5 (e), 10 (f), 25 (g), 50 (b, h), and 100 μM (i). Lanes k and m contain 50 μM echinomycin; Lanes j and l contain 50 μM distamycin. The numbering corresponds to the sequence shown in Figure 1. The track labeled "G" is a Maxam–Gilbert dimethyl sulfate–piperidine marker specific for guanine.

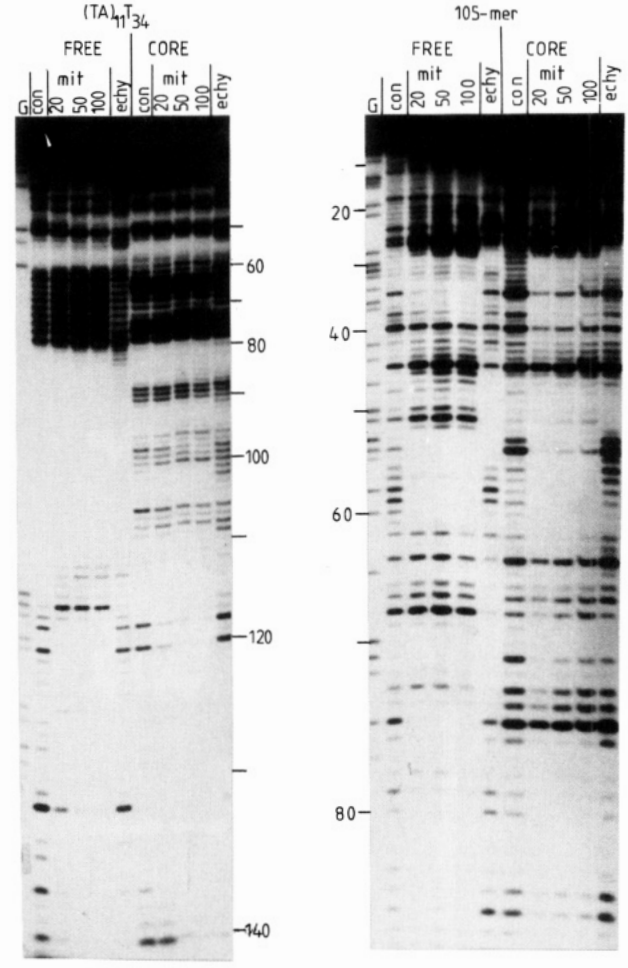

FIGURE 8: DNase I digestion of $(TA)_{11}T_{34}$ and 105-mer, free and complexed with nucleosome cores, in the presence and absence of mithramycin and echinomycin. Tracks labeled "con" correspond to the control in the absence of ligand. Mithramycin concentrations (in micromolar) are shown at the top of each lane; the tracks labeled "echy" correspond to 50 μM echinomycin. The numbering corresponds to the sequence shown in Figure 1. The track labeled "G" is a Maxam–Gilbert dimethyl sulfate–piperidine marker specific for guanine.

40, 49–51, 59, 82, 97, and 110, whereas for distamycin novel cleavage products are found around positions 55, 65, 76, 97, and 119. In both cases, the pattern has been explained by suggesting that the antibiotics have caused the DNA to rotate by 180° on the protein surface, so that regions which were originally facing toward the core are now exposed to digestion by DNase I.

$(AT)_{11}T_{34}$. Figure 8 presents DNase I digestion patterns for a human genomic clone containing the sequence $(AT)_{11}T_{34}$ in the presence and absence of mithramycin and echinomycin. The sequence of this DNA is shown in Figure 1; the DNase I digestion pattern of this fragment when complexed with nucleosome core particles has previously been described (Fox, 1992). Since this DNA contains a long stretch of AT residues, which exhibit a clear phasic pattern, and to which mithramycin and echinomycin do not bind, it provides an ideal substrate for examining the effects of these antibiotics on DNA rotation. Although the 3′-end of this fragment is fairly GC-rich, it contains only two echinomycin CG binding sites at positions 127 and 146. On the free DNA, mithramycin produces clear footprints around positions 118–123 (GGCC) and 126–131 (GGCGGGC). Surprisingly, there is no footprint around the GGG which is immediately distal (below) to the T tract, although cleavage is enhanced at the 3′-end of this tract. When this DNA is complexed with the core particle, the DNase I pattern in the absence of drugs changes dramatically. Whereas the T_{34} tract is virtually uncut in the control, a phased pattern of cleavage products is apparent in the core-bound sample in which the intensity of the strongly cut bands is similar to that

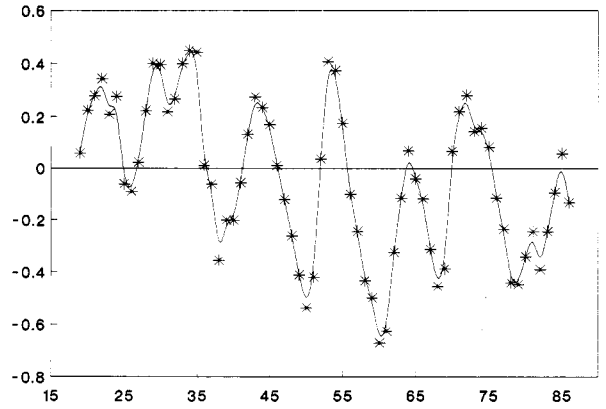

FIGURE 9: Differential cleavage plots showing DNase I cleavage of the 105-mer when complexed to nucleosome core particles compared with that of free DNA. Each point corresponds to the logarithm of the relative cleavage; negative values indicate regions protected by the core particles. The abscissa corresponds to the numbering in Figure 1.

in the rest of the fragment (Fox, 1992). Our previous studies have shown that the minor groove faces away from the core at positions 64, 76, 88–90, 97–99, and 106–108; this phasic pattern continues in the remainder of the fragment, and further strong bands are apparent at positions 118–120, 128–129, and 138–140 in the core-bound DNA, suggesting that these regions are located with their minor grooves facing away from the protein core. Low concentrations of mithramycin (20 μM) protect positions 128–129 from cleavage; higher concentrations are required to protect positions 118–120. Since these sites face away from the core, they should both be accessible to mithramycin binding. More importantly, the pattern of cleavage within the long AT tract remains essentially the same in the presence of the antibiotic, although some changes in the relative band intensity are evident in the center of this region around position 100. We can confidently assert that mithramycin has not affected the orientation of this DNA region on the core particle. In contrast, the only canonical echinomycin binding site (CpG) is located at position 127, and produces a clear footprint in the free DNA. Cutting of this region is poor in the core-bound DNA so that it is not possible to rigorously analyze echinomycin binding. The phased cleavage pattern of the T_{34} tract is retained in the presence of echinomycin, confirming that the DNA is still associated with the core particles and that the antibiotic has not provoked any major changes in its orientation. However, despite the lack of any clear echinomycin footprints, some drug-induced changes can be seen in the cutting pattern of the T_{34} tract. These may arise from weaker drug binding to $(AT)_n$, as previously described (Fox et al., 1992).

105mer. DNase I cleavage patterns for the 105 base pair DNA fragment, both free and complexed with nucleosome core particles, are presented in Figure 8. Inspection of these patterns reveals reduced cleavage of the core-bound DNA around positions 25, 36, 47, 58, 67, and 77 and strong cutting around positions 21, 33, 43, 52, 64, and 71; these must correspond to regions where the minor groove faces toward and away from the protein core, respectively. These data are presented in the form of a differential cleavage plot (Drew & Travers, 1985) in Figure 9 and show the cutting of the core-bound DNA relative to that of the free DNA. Between positions 21 and 85 there are 6 peaks, indicating a periodicity of 64/6 = 10.6 base pairs. These data suggest that this DNA has been successfully reconstituted with nucleosome cores and adopts a defined orientation on the protein surface.

Mithramycin produces clear footprints on the free DNA around positions 70–84, 53–61, and 34–38, the first two of which correspond to several overlapping sites. When this DNA is complexed with nucleosome core particles, mithramycin induces a DNase I digestion pattern which is different from both the free DNA, in the presence or absence of the antibiotic, and the core-bound DNA. Mithramycin-induced footprints on this core DNA are evident at positions 76–83, 47–62, and 36–40 with a weaker site between 69 and 74. The region around position 75, which was protected in the free DNA, is still efficiently cleaved in the nucleosomal DNA. The footprint between 47 and 62 appears to be much larger than that found in the free DNA, which only extends from 53 to 61. However, the upper portion of this footprint cannot be rigorously assigned since DNase I cleavage is already significantly reduced as the minor groove faces toward the protein core. The footprint at 34–38 on free DNA is replaced by protection between 36–40 and 28–35. These will be considered further under Discussion, but it is clear that although mithramycin has not displaced the DNA from the protein core its binding sites have been modified by the interaction with the protein.

The only echinomycin binding sites (CG) on this fragment, at positions 87 and 92, run off the bottom of the gel. Nevertheless, echinomycin also protects the free DNA from cleavage between positions 46–54 and 66–73. These probably correspond to secondary echinomycin binding sites, possibly to the TpG steps. Echinomycin has no effect on DNase I digestion of this fragment when complexed with nucleosome core particles, suggesting that these secondary sites are no longer available, either due to changes in their conformation or due to steric hindrance from the protein core itself.

DISCUSSION

Mithramycin. The results presented in this paper demonstrate that mithramycin interacts with nucleosome-bound DNAs in a sequence-selective fashion and does so without affecting the integrity of the nucleosome. Mithramycin produces clear footprints with all the DNA fragments investigated and does not disrupt the phased cleavage pattern. While this may not seem surprising, it stands in contrast to results for several other ligands. Actinomycin and nogalamycin cause DNA to dissociate from the core particles (Portugal & Waring, 1987), while echinomycin and distamycin have been reported to cause DNA to rotate by 180° on the protein surface (Low et al., 1986; Portugal & Waring, 1986).

Several studies have shown that mithramycin binds as a dimer, widening the DNA minor groove so that it more closely resembles an A-DNA helix. Does this model give any clues concerning the ways in which mithramycin might interact with nucleosome-bound DNAs? In general, GC-rich sequences possess a wider than average minor groove and are therefore preferentially located with their minor grooves facing away from the protein core (Drew & Travers, 1985). As a result, many GC-rich mithramycin binding sites should be positioned with their minor grooves readily accessible. These regions will already possess a wider than average minor groove, and so should therefore represent ideal mithramycin binding sites. Indeed, it may be that the mithramycin-induced structural changes, which are often observed as enhanced rates of nuclease cleavage, may not be so apparent since the DNA more closely resembles the correct structure for ligand binding and so does not need to be further distorted.

In contrast to distamycin and echinomycin, mithramycin produces discrete footprints on these nucleosome-bound DNAs, which are a subset of the regions protected on free

DNA. Although echinomycin and distamycin induce large changes in DNase I cleavage patterns, these are not centered around discrete footprints. Low et al. (1986) have suggested that this may be because only a few ligands need to bind to cause the structural changes; if these are randomly distributed among the potential ligand binding sites, then the fractional occupancy at each site may not be sufficient to produce a discrete footprint. The clear footprints induced by mithramycin must therefore indicate a relatively high level of occupancy at each site, suggesting that nucleosomal DNA may be able to tolerate a greater level of mithramycin binding than either distamycin or echinomycin.

Although mithramycin produces clear footprints on DNA fragments which are complexed with nucleosome cores, and many of these sites correspond to those seen with free DNA, some regions no longer bind the antibiotic. This is evident for *tyr*T DNA at positions 103–110, and for the 135mer at positions 48–50 and 75–83. This difference can be explained in two ways. Either the sites are occluded by the protein core, i.e., the minor groove faces toward the nucleosome, or the local DNA structure has been modified so that it can no longer accommodate mithramycin. We favor the second possibility for several reasons. First, some sites which are not occupied in core DNA are positioned with their minor grooves facing away from the nucleosome cores, and should be readily accessible to the antibiotic. This can be seen around 103–110 in *tyr*T DNA; this contains the sequence CCCG and is centered on a region in which the minor groove is on the outer surface of the supercoil. Second, an explanation in terms of altered DNA structure more readily accounts for the new footprints seen on the core-bound fragments only, and is consistent with other studies which have shown that the binding of mithramycin is dependent on the nature of the surrounding sequences. An example of these novel DNase I footprints on nucleosomal DNA can be seen at positions 60–63 on the 135mer. This region contains the sequence GCC, and might have been expected to bind the ligand on free DNA. We therefore suggest that this site was not occupied in free DNA because of some aspect of the local DNA structure, possibly a narrow minor groove which is not easily widened to accommodate the ligand. When it is wrapped around nucleosome cores, it is positioned on the outer surface of the DNA supercoil and is forced to adopt a wider minor groove which more readily binds the antibiotic.

Against this background, it is surprising that mithramycin does not produce discrete hydroxyl radical footprints on the core-bound DNAs. However, it should be remembered that the absence of hydroxyl radical footprints does not necessarily indicate a lack of sequence-specific binding. Several sequence-specific drugs, most notably actinomycin, do not yield hydroxyl radical footprints.

Although mithramycin does not disrupt the positioning of DNA on the nucleosome cores, it does cause some local changes in the nucleosomal cleavage pattern. This can be seen most clearly in the T_{34} tract in Figure 8. In the control, the strongest bands are at positions 106, 98, and 88–90 with much weaker cleavage to either side. In the presence of mithramycin, the strongest products are found at positions 100, 108, 106, 96, and 78–80. Cleavage in the adjoining $(AT)_{11}$ tract is unaffected. The closest mithramycin binding site is the sequence GGG located immediately 3′ to the T tract. By binding to this site, which is not occupied in the free DNA, mithramycin alters the fine details of the interaction of the T_{34} tract with the nucleosome. This may be related to the known ability of mithramycin to alter the structure of adjacent A_n·T_n, rendering it more like B-DNA (Cons & Fox, 1991). Since the phasing in the remainder of this fragment is unaffected, these DNA structural changes must be accommodated within the existing overall nucleosome structure. This may be achieved locally by loosening the interaction between the DNA and the protein core, causing the formation of small local loops and buckles. We have previously suggested (Fox, 1992) that this DNA fragment does not wrap evenly around the nucleosome core, as evidenced by variations in the distance between peaks in the DNase I cleavage pattern, and that these small local variations may be dictated by the way in which the protein core distorts the T_{34} tract. If the structure of this DNA region is altered by drug binding, then the precise location of the bends will also be affected.

Distamycin and Echinomycin. Previous studies have suggested that these ligands cause DNA to rotate by 180° on the protein surface, evidenced by the presence of new DNase I digestion products, located midway between the existing maxima (Low et al., 1986; Portugal & Waring, 1986). Although we confirm these observations, the hydroxyl radical and DEPC data do not provide evidence for this rotation, but rather suggest that nucleosome positioning is unchanged. Indeed, the echinomycin-induced DEPC cleavage pattern, in which adenines distal to CpG become hyperreactive, is still observed in core-bound DNA, confirming that this structural change can be accommodated within the nucleosome structure.

The results presented in this paper confirm that echinomycin and distamycin can bind to nucleosomal DNA, unlike actinomycin and nogalamycin, but do so without radically altering the rotational positioning of the DNA. Although this may seem reasonable, it leaves the question of what is responsible for the novel DNase I cleavage products observed with these ligands on several DNA fragments. The explanation may be different for the two ligands which bind to DNA by dissimilar mechanisms. We shall first consider echinomycin. This bifunctional intercalator unwinds DNA by 48°, so that there must be a local change in nucleosome structure. Since the binding site size of the drug is four base pairs, the average local helical twist in the presence of the ligand will be 34–48/4, i.e., 22°. Insertion of the 2 quinoxaline chromophores will also lengthen the DNA helix by the equivalent of 2 base pairs, so that, given an optimal arrangement of binding sites, the distance originally occupied by 1 turn of the helix (10 base pairs) will now be covered by only 5 base pairs. It is therefore obvious that the ligand must disrupt the regular arrangement of DNA around the core particles. This will be further complicated since the drug–DNA complex will be more rigid and unable to wrap smoothly around the cores. This is supported by the observation that echinomycin does not produce clear DNase I footprints on nucleosomal DNA, and has previously been explained by suggesting that only one or two drug molecules can be tolerated within the core sequence; addition of further molecules disrupts the nucleosome structure. Inspection of the novel cleavage products found in the presence of echinomycin reveals that, although they appear to be spaced at regular intervals, midway between the previous maxima, they are not all of equal intensity. Moreover, the previously strong bands, indicating the rotational positioning of the DNA, are still evident. We therefore suggest that the new DNase I cleavage products do not correspond to DNA rotation, but to some distortion of the DNA helix as it accommodates to the locally bound drug molecule. As a result, the DNA may not wrap smoothly around the nucleosome but may be forced to adopt kinks and buckles, as the novel structures are accommodated within the existing protein–

DNA complex. As previously noted, most of the potential echinomycin CG sites are located with their minor groove facing away from the protein core; if drug-induced structural adaptations are located in adjacent regions, then these will be in regions which the minor groove is usually protected, facing the protein core. These subtle variations can be seen in the DNase I cleavage patterns of T tract in the fragment containing the sequence $(TA)_{11}T_{34}$. Although the peaks are found in similar locations to that of the core DNA without antibiotic, echinomycin has altered the precise local pattern. The closest echinomycin (CG) binding site is located 14 bases to the 3′-side of the T tract; it therefore seems unlikely that this is responsible for these changes, especially since cleavage of the intervening bases is largely unchanged. A more plausible explanation is that there is some, albeit weak, interaction of echinomycin with the $(AT)_n$ tract (Fox et al., 1992), causing structural changes which affect the precise interaction of the T tract with the nucleosome core.

We cannot offer an alternative explanation for bands produced by distamycin and other minor groove binding agents. These drugs do not unwind DNA, but may cause a slight overwinding (Snounou & Malcolm, 1983). Maybe their effects are related to the requirement for binding to a narrow minor groove, possibly causing a stiffening of the DNA helix.

Mithramycin is the only sequence-selective drug so far investigated which yields clear footprints on nucleosomal DNA, suggesting that full occupancy of each site can be tolerated within the nucleosome structure. Mithramycin does not unwind or lengthen the DNA helix, and, since its minor groove binding sites should be located on the outside of the DNA supercoil, it may be much better tolerated within nucleosomal DNA, than many other agents, including echinomycin and distamycin. If this argument is correct, then the best agents for binding to nucleosomal DNA should be nonintercalators which bind either to the GC-rich minor groove or to an AT-rich major groove. We are not aware of any small ligands in the latter category.

REFERENCES

Banville, D. L., Keniry, M. A., Kam, M., & Shafer, R. H. (1990a) *Biochemistry 29*, 6521–6534.

Banville, D. L., Keniry, M. A., & Shafer, R. H. (1990b) *Biochemistry 29*, 9294–9304.

Cons, B. M. G., & Fox, K. R. (1989a) *Biochem. Biophys. Res. Commun. 160*, 517–524.

Cons, B. M. G., & Fox, K. R. (1989b) *Nucleic Acids Res. 17*, 5447–5459.

Cons, B. M. G., & Fox, K. R. (1990a) *FEBS Lett. 264*, 100–104.

Cons, B. M. G., & Fox, K. R. (1990b) *Anti-Cancer Drug Des. 5*, 93–97.

Cons, B. M. G., & Fox, K. R. (1991) *Biochemistry 30*, 6314–6321.

Drew, H. R., & Travers, A. A. (1985) *J. Mol. Biol. 186*, 773–790.

Drew, H. R., & Calladine, C. R. (1987) *J. Mol. Biol. 195*, 143–173.

Fox, K. R. (1992) *Nucleic Acids Res. 20*, 1235–1242.

Fox, K. R., & Waring, M. J. (1984) *Nucleic Acids Res. 12*, 9271–9285.

Fox, K. R., & Howarth, N. R. (1985) *Nucleic Acids Res. 13*, 8695–8714.

Fox, K. R., & Kentebe, E. (1990) *Biochem. J. 269*, 217–221.

Fox, K. R., Marks, J. N., & Waterloh, K. (1992) *Nucleic Acids Res. 24*, 6725–6730.

Gao, X., & Patel, D. J. (1989) *Biochemistry 28*, 751–762.

Gao, X., & Patel, D. J. (1990) *Biochemistry 29*, 10940–10956.

Gao, X., Mirau, P., & Patel, D. J. (1992) *J. Mol. Biol. 223*, 259–279.

Gause, G. F. (1975) in *Antibiotics III, Mechanism of Action of Antimicrobial and Antitumour Agents* (Corcoran, J. W., & Hahn, F. E., Eds.) pp 197–202, Springer-Verlag, Berlin, Heidelberg, and New York.

Hayes, J. J., Tullius, T. D., & Wolffe, A. P. (1990) *Proc. Natl. Acad Sci. U.S.A. 87*, 7405–7409.

Hayes, J. J., Clark, D. J., & Wolffe, A. P. (1991a) *Proc. Natl. Acad. Sci. U.S.A. 88*, 6829–6833.

Hayes, J. J., Bashkin, J., Tullius, T. D., & Wolffe, A. P. (1991b) *Biochemistry 30*, 8434–8440.

Kersten, W., Kersten, H., & Szybalski, W. (1966) *Biochemistry 5*, 236–244.

Low, C. M. L., Drew, H. R., & Waring, M. J. (1986) *Nucleic Acids Res. 14*, 6785–6801.

Mendel, D., & Dervan, P. B. (1987) *Proc. Natl. Acad. Sci. U.S.A. 84*, 910–914.

Portugal, J., & Waring, M. J. (1986) *Nucleic Acids Res. 14*, 8735–8754.

Portugal, J., & Waring, M. J. (1987a) *Nucleic Acids Res. 15*, 885–903.

Portugal, J., & Waring, M. J. (1987b) *Eur. J. Biochem. 167*, 281–289.

Portugal, J., & Waring, M. J. (1987c) *FEBS Lett. 225*, 195–200.

Portugal, J., Fox, K. R., McLean, M. J., Richenberg, J. L., & Waring, M. J. (1988) *Nucleic Acids Res. 16*, 3655–3670.

Ray, R., Snyder, R. C., Thomas, S., Koller, C. A., & Miller, D. M. (1989) *J. Clin. Invest. 83*, 2003–2007.

Schrader, T. E., & Crothers, D. M. (1989) *Proc. Natl. Acad. Sci. U.S.A. 86*, 7418–7422.

Schrader, T. E., & Crothers, D. M. (1990) *J. Mol. Biol. 216*, 69–84.

Snounou, G., & Malcolm, A. D. B. (1983) *J. Mol. Biol. 167*, 211–216.

Snyder, R. C., Ray, R., Blume, S., & Miller, D. M. (1991) *Biochemistry 30*, 4290–4297.

Van Dyke, M. W., & Dervan, P. B. (1983) *Biochemistry 22*, 2373–2377.

Waring, M. J. (1970) *J. Mol. Biol. 54*, 247–279.